Available online at www.sciencedirect.com

ScienceDirect

Geochimica et Cosmochimica Acta 201 (2017) 364–376

Geochimica et Cosmochimica Acta

www.elsevier.com/locate/gca

Calcium isotopic compositions of chondrites

Shichun Huang [a,*], Stein B. Jacobsen [b]

[a] Department of Geoscience, University of Nevada, Las Vegas, United States
[b] Department of Earth and Planetary Sciences, Harvard University, United States

Received 16 March 2016; accepted in revised form 29 September 2016; available online 4 October 2016

Abstract

We report mass-dependent and mass-independent Ca isotopic variations in nine chondrites from three groups: carbonaceous, ordinary and enstatite chondrites. There is about 0.25‰ per amu, i.e., ~1‰ in $^{44}Ca/^{40}Ca$, variation in chondrites: carbonaceous chondrites have the lightest Ca isotopes, enstatite chondrites have modeled bulk Earth like Ca isotopes, and ordinary chondrites are in between. The correlations between mass-dependent Ca isotopic variation and chemical variations in chondrites may reflect variable contributions from different endmembers, including refractory inclusions, in different chondrite groups. In detail, enstatite chondrites and the Earth share similar isotopic characteristics, but are very different in chemical compositions.

At the ±1 and ±2 ε-unit levels, respectively, there is no measurable ^{40}Ca or ^{43}Ca anomaly in bulk chondrites. Carbonaceous chondrites show several ε-units of ^{48}Ca excess. That is, Ca exhibits both mass-dependent and mass-independent isotopic variations in chondrites, similar to O isotopes. The ^{48}Ca anomaly in bulk chondrites is positively correlated with ^{50}Ti anomaly, but does not form simple correlation with ^{54}Cr anomaly, implying multiple supernova sources for these neutron-rich isotopes in the Solar System. Finally, all meteorites with negative $\Delta^{17}O$ have either ^{48}Ca deficits (differentiated meteorites) or ^{48}Ca excess (carbonaceous chondrites), implying that the Sun with a very negative $\Delta^{17}O$ is probably also characterized by ^{48}Ca anomaly compared to the Earth. CAIs cannot be taken as representative of the initial isotopic compositions of refractory elements like Ca for the Earth–Moon system.

Keywords: Chondrites; Calcium isotopes; Nucleosynthetic anomaly; Double spike

1. INTRODUCTION

Primitive meteorites, i.e., chondrites, escaped parental body differentiation processes, and are thought to be representative of the "building-blocks" of the planets in our Solar System (e.g., Jacobsen and Wasserburg, 1980). Their isotopic and chemical compositions provide important constraints on the formation and evolution of the early Solar System. It has been known for several decades that chondrites show very large O isotopic variations, both mass-dependent and mass-independent, and that only enstatite chondrites and the Earth share the same O isotopic characteristics (e.g., Clayton, 2003). While Mg and Fe isotopic studies show that all chondrites and the Earth share the same isotopic compositions (e.g., Poitrasson et al., 2005; Schoenberg and von Blanckenburg, 2006; Teng et al., 2008, 2010; Chakrabarti and Jacobsen, 2010a; von Strandmann et al., 2011), Si is more complicated due to conflicting results in the literature (Georg et al., 2007; Fitoussi et al., 2009; Ziegler et al., 2010; Chakrabarti and Jacobsen, 2010b; Armytage et al., 2011; Fitoussi and Bourdon, 2012; Savage and Moynier, 2013). In detail,

* Corresponding author.
E-mail addresses: shichun.huang@unlv.edu (S. Huang), jacobsen@neodymium.harvard.edu (S.B. Jacobsen).

http://dx.doi.org/10.1016/j.gca.2016.09.039
0016-7037/

ordinary and carbonaceous chondrites have similar Si isotopic compositions, which are slightly heavier than enstatite chondrites, a difference attributed to lighter Si isotopes in the metal phase in enstatite chondrites (e.g., Shahar et al., 2011; Savage and Moynier, 2013). In contrast, Dauphas et al. (2015) argued that the Si isotopic variations in chondrites reflect equilibrium Si isotopic fractionation between solid olivine and gaseous SiO in the Solar nebula. The reported Si isotopic difference between the Earth and the (ordinary and carbonaceous) chondritic average ranges from non-resolvable to 0.1‰ per amu, which may reflect lighter Si isotopes in the Earth's core (e.g., Georg et al., 2007) or lower mantle (Huang et al., 2014).

Based on atoms per 10^6 Si atoms, Ca is the sixth most abundant element in rocky planets and chondrites, after O, Si, Mg, Fe and Al (e.g., Anders and Grevesse, 1989). Ca has a rich isotope system: It consists of six stable isotopes, ranging from mass 40 to 48, the third largest relative mass difference only after H and He. According to Burbidge et al. (1957), ^{40}Ca is generated during the oxygen- and silicon-burning processes, and it is also one of the decay products of ^{40}K ($t_{1/2} = 1.27$ Ga). ^{42}Ca and ^{43}Ca are produced during the oxygen-burning process. ^{44}Ca is the decay product of the short-lived ^{44}Ti ($t_{1/2} = 60$ yrs), which is produced together with ^{40}Ca during oxygen- and silicon-burning processes. ^{46}Ca is an s-process isotope. ^{48}Ca requires a special neutron-rich nucleosynthetic process, which might happen during Type Ia supernova explosion (Meyer et al., 1996) and electron-capture supernova explosion (Wanajo et al., 2013). What are the Ca isotopic signatures of chondrites and their relationship to the Earth, other rocky planets and asteroids? Existing Ca isotopic studies on bulk chondrites focused on mass-dependent isotopic variations (Simon and DePaolo, 2010; Valdes et al., 2014) which yield different results on enstatite chondrites, and some mass-independent isotopic variations are reported on a subset of chondrites (Simon et al., 2009; Moynier et al., 2010; Dauphas et al., 2014; Schiller et al., 2015). Here we report both mass-dependent and mass-independent Ca isotopic measurements on nine chondrites from all three major chondrite groups, carbonaceous, ordinary and enstatite chondrites.

2. SAMPLES AND ANALYTICAL PROCEDURE

Nine chondrites from three groups were selected for Ca isotopic measurements, including three carbonaceous chondrites: Allende (CV3), Murchison (CM2) and Orgueil (CI1); four ordinary chondrites: Bruderheim (L6), Peace River (L6), Grady (1937) (H3) and Guarena (H6); and two enstatite chondrites: Abee and Indarch (both are EH). In addition, a lunar anorthosite, 60025, and a eucrite, Juvinas, are also analyzed for comparison.

The detailed analytical procedure, including sample dissolution, Ca column chemistry, and TIMS measurements, has been documented in our previous publications (Huang et al., 2010, 2011, 2012). Here we provide a short summary. Several mg of powdered samples were dissolved using 2 ml 1:1 mixed HF-HNO_3 acid in capped 6 ml standard square body Teflon vials at 120 °C for two weeks. Then the sample solutions were dried down three times with concentrated HNO_3 and once with concentrated HCl to break down the insoluble CaF_2. Finally, the sample was diluted using 2.5 N HCl to form a 10 μg Ca/μl solution. For unspiked TIMS measurement, Ca was purified from each sample solution using HCl on a cation column (BioRad AG50W-X12). For spiked TIMS measurement, a certain amount of ^{43}Ca–^{48}Ca double spike solution was mixed with each sample solution before column chemistry. Our column chemistry was carefully calibrated to ensure ~100% Ca yield, and each sample was passed through the column twice to ensure that the final Ca cut is free of matrix elements, such as K and Ti. For each measurement, ~5 μg of purified Ca was loaded as $Ca(NO_3)_2$ onto one of the side filaments of a zone-refined Re triple filament assembly. The Ca isotopic ratios were measured using a GV Isoprobe-T TIMS at Harvard University, with a two-sequence method: the first sequence collects ^{40}Ca, ^{41}K, ^{42}Ca, ^{43}Ca and ^{44}Ca, and the second collects ^{44}Ca and ^{48}Ca. Prior to data acquisition, masses 43.5, 47 and 49 have been carefully scanned using electron multiplier to ensure that no doubly charged ^{87}Sr, ^{47}Ti and ^{49}Ti signals were observed. The measured sample-to-spike ratios, ^{40}Ca/^{48}Ca, in all our spiked measurements are within 5% of that obtained using the weights of the dissolved samples, their CaO contents, and the ^{43}Ca-^{48}Ca double spike amounts, indicating that undissolved Ca-bearing phase, if any, is negligible in all our samples. Because of the 10 V limit of the Faraday cups on our Isoprobe-T TIMS, the internal precision is much better than external reproducibility. Consequently, each sample was measured multiple times, and the averages and resulting external reproducibility are reported.

Two types of Ca isotopic variations are reported. Compared to terrestrial silicate rocks and minerals, SRM915a does not show any measurable radiogenic ^{40}Ca excess at ±0.5 ε-unit level (Amini et al., 2009; Simon et al., 2009; Caro et al., 2010; Table 1). Consequently, in this paper SRM915a is used as the standard sample reporting both mass-dependent and mass-independent Ca isotopic effects. For mass-independent Ca isotopic variation, both instrumental and natural mass fractionations are corrected using the exponential law to a constant ^{42}Ca/^{44}Ca ratio of 0.31221 (Russell et al., 1978), and mass-independent Ca isotopic variations are reported using ε-notation:

$$\varepsilon^{4i/44}\mathrm{Ca} = \left[\frac{(^{4i}\mathrm{Ca}/^{44}\mathrm{Ca})_{\mathrm{sample(N)}}}{(^{4i}\mathrm{Ca}/^{44}\mathrm{Ca})_{\mathrm{SRM915a(N)}}} - 1\right] \times 10{,}000$$

where i represents 40, 43 and 48, and (N) in the subscript denotes value obtained after internal normalization. Thirty-two measurements of NIST SRM915a yield ^{40}Ca/^{44}Ca = 47.134 ± 0.002, ^{43}Ca/^{44}Ca = 0.064950 ± 0.000004, and ^{48}Ca/^{44}Ca = 0.088691 ± 0.000004 (all $2\sigma_m$), after internal normalization to ^{42}Ca/^{44}Ca = 0.31221.

For mass-dependent Ca isotopic variation, the instrumental mass fractionation is corrected using a ^{43}Ca–^{48}Ca double spike technique, as described in detail in Huang et al. (2010, 2011, 2012), so that natural isotopic variations can be measured. Mass-dependent Ca isotopic variation is reported using δ-notation:

Table 1
Ca isotope compositions of primitive meteorites, eucrite (Juvinas), and lunar anorthosite (60025).

									Age-corrected								
		$\delta^{44/40}Ca$	$2\sigma_m$	$\delta^{42/40}Ca$	$2\sigma_m$	$\delta^{44/42}Ca$	$2\sigma_m$	n	$\delta^{44/40}Ca$	$\delta^{42/40}Ca$	$\varepsilon^{40/44}Ca$	$2\sigma_m$	$\varepsilon^{43/44}Ca$	$2\sigma_m$	$\varepsilon^{48/44}Ca$	$2\sigma_m$	n
Chondrites																	
Murchison	CM2	0.72	0.04	0.38	0.03	0.34	0.05	6			−0.4	0.6	0.4	0.6	2.1	0.9	8
Orgueil	CI1	0.75	0.08	0.36	0.05	0.40	0.05	5			0.9	1.0	−0.3	2.1	2.3	0.8	5
Allende	CV3	0.28	0.05	0.14	0.05	0.14	0.02	6			−0.5	0.5	0.2	0.9	2.9	0.6	12
Bruderham	O, L6	0.98	0.07	0.51	0.06	0.47	0.04	8			0.2	0.3	0.0	2.4	0.4	0.8	12
Peace River	O, L6	0.83	0.11	0.43	0.11	0.40	0.09	5			0.0	0.6	0.4	1.2	−0.2	1.2	9
Guarena	O, H6	0.91	0.03	0.43	0.06	0.47	0.05	4			−0.4	0.7	0.1	1.1	−0.3	1.0	8
Grady (1937)	O, H3	0.92	0.04	0.49	0.03	0.44	0.03	6			0.7	0.7	0.0	1.1	0.4	0.7	8
Abee	EH	0.90	0.02	0.38	0.04	0.52	0.03	6	1.02	0.50	0.6	0.5	−0.1	1.3	−0.9	1.3	12
Indarch	EH	0.96	0.02	0.44	0.04	0.52	0.04	7	1.06	0.54							
Eucrite																	
Juvinas											−0.5	0.5	−0.2	1.4	−1.6	1.0	13
Moon																	
60025											−0.3	1.4	−1.7	1.6	−0.1	1.8	7
Terrestrial basalts and silicate minerals																	
BHVO-1											0.6	0.6	0.0	0.9	1.0	1.0	9
BCR-1											−0.1	0.6	−0.6	1.2	0.2	1.1	9
Kilbourne Hole clinopyroxene											−0.5	1.1	−1.2	1.9	−1.2	1.4	4
San Carlos clinopyroxene											−0.2	0.5	1.1	1.4	0.1	0.8	12
San Carlos orthopyroxene											−0.3	0.7	−0.5	1.2	−0.5	0.9	5
Standards																	
Sea Water		1.87	0.02	0.91	0.03	0.96	0.02	42			−0.4	0.6	−0.6	1.2	0.0	1.0	14
NIST SRM 915a		−0.02	0.02	−0.04	0.03	0.02	0.03	43			0.0	0.4	0.0	0.7	0.0	0.5	32

See text for definition of δ and ε values, and analytical uncertainty.

$$\delta^{4i/4j}Ca = \left[\frac{(^{4i}Ca/^{4j}Ca)_{sample}}{(^{4i}Ca/^{4j}Ca)_{SRM915a}} - 1\right] \times 1,000$$

where $4i$ and $4j$ represent 40, 42 and 44. Combined spiked and unspiked measurements of NIST SRM915a yield $^{40}Ca/^{44}Ca$ of 46.406 ± 0.001 and $^{42}Ca/^{44}Ca$ of 0.30985 ± 0.00001 (all $2\sigma_m$), which are used as normalization values to calculate the δ-values. The reproducibility of $\delta^{44/40}Ca$ in seawater and NIST SRM 915a over the past 7 years is shown in Fig. 1. This work was all done with the same Faraday cups since the instrument was delivered in 2005.

3. RESULTS

The mass-dependent and mass-independent Ca isotopic variations of chondrites are given in Table 1. The mass-dependent Ca isotopic variations of chondrites are shown in two Ca three-isotope plots, $\delta^{44/40}Ca$ vs. $\delta^{42/40}Ca$ and $\delta^{44/42}Ca$ (Fig. 2). After correction for radiogenic ^{40}Ca ingrowth in two enstatite chondrites, all nine chondrites plot on the mass-dependent fractionation trends, with $\delta^{44/40}Ca_{SRM915a}$ ranging from 0.28 to 1.06. Such variation is comparable to that observed in terrestrial silicate rocks, 0.2–1.9 (Fantle and Tipper, 2014), and twice as that observed in martian meteorites, 0.7–1.1 (Magna et al., 2015). Because of the limited $\delta^{44/40}Ca$ range in these chondrites, the observed $\delta^{44/40}Ca$ vs. $\delta^{42/40}Ca$ and $\delta^{44/42}Ca$ chondrite trends are consistent with several types of fractionation laws, including the exponential law (Fig. 2). The low-$\delta^{44/40}Ca_{SRM915a}$ end is defined by carbonaceous chondrites, the high-$\delta^{44/40}Ca_{SRM915a}$ end by enstatite chondrites which overlap with the estimate of the Earth based on peridotites (1.05; Huang et al., 2010), and ordinary chondrites are in between these two chondritic groups.

Our unspiked measurements show that at about ±1 and ±2 ε-unit levels, respectively, there are no measurable isotopic anomalies on ^{40}Ca or ^{43}Ca in bulk chondrites, lunar anorthosite 60025 and eucrite Juvinas (Table 1; Fig. 3). In detail, lunar anorthosite 60025 has a $\varepsilon^{43/44}Ca$ of -1.7 ± 1.6, which is indistinguishable from the measured standard value 0.0 ± 0.7 (Table 1). Ordinary and enstatite chondrites do not show any measurable ^{48}Ca anomaly, and all three carbonaceous chondrites show 2–3 ε-units of ^{48}Ca excess. This result is similar to Ca isotopic studies of refractory inclusions, which did not show measurable mass-independent isotopic variations on ^{40}Ca or ^{43}Ca, but several ε-units of ^{48}Ca excess (Lee et al., 1978, 1979; Jungck et al., 1984; Niederer and Papanastassiou, 1984; Ireland et al., 1992; Moynier et al., 2010; Huang et al., 2012). There is no measurable ^{48}Ca anomaly in lunar anorthosite 60025; however, the eucrite Juvinas has a negative ^{48}Ca anomaly with $\varepsilon^{48/44}Ca$ of -1.6 ± 1.0 (Table 1).

4. DISCUSSION

4.1. Inter-lab comparison

Calcium isotopic compositions, both mass-dependent and mass-independent, of chondrites have been measured by several groups. A comparison with published data is necessary. Fig. 3a shows a comparison of our $\delta^{44/40}Ca$ values with published values from Simon and DePaolo (2010), who used a ^{42}Ca–^{48}Ca double spike TIMS technique, and Valdes et al. (2014) and Schiller et al. (2015), both used a sample-standard bracketing technique on a MC-ICP-MS. Because Valdes et al. (2014) and Schiller et al. (2015) could not measure $\delta^{44/40}Ca$ directly, they reported $\delta^{44/42}Ca$ data, and the $\delta^{44/40}Ca$ values were calculated by multiplying their reported $\delta^{44/42}Ca$ values by two. All published data have been renormalized to SRM915a for comparison. In general, results from three groups agree with each other. However, important discrepancies include:

a. Allende: Our Allende $\delta^{44/40}Ca$ value, 0.28 ± 0.05, is lower than that by Simon and DePaolo (2010) and Valdes et al. (2014), 0.54 ± 0.05 and 0.55 ± 0.10, respectively. This probably reflects sample heterogeneity, caused by inhomogeneous distribution of refractory inclusions in Allende.

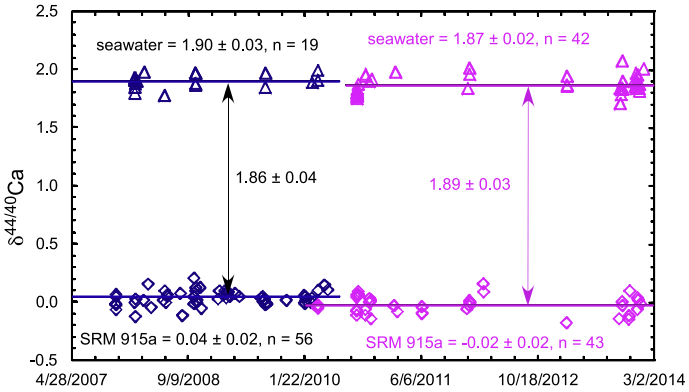

Fig. 1. Reproducibility of $\delta^{44/40}Ca$ for seawater and NIST SRM 915a measured with the IsoProbe-T TIMS at Harvard University since 2007. This work was all done with the same Faraday cups since the instrument was delivered in 2005. The cited errors are $2\sigma_m$ of multiple analyses. Two ^{43}Ca–^{48}Ca double spike solutions have been used during the course of our analyses (see Huang et al., 2011 for a detailed discussion). $\delta^{44/40}Ca_{SRM915a}$ of two standard samples measured using these two spikes agree within analytical uncertainty. There is no long-term $\delta^{44/40}Ca_{SRM915a}$ drift in our measured standard samples.

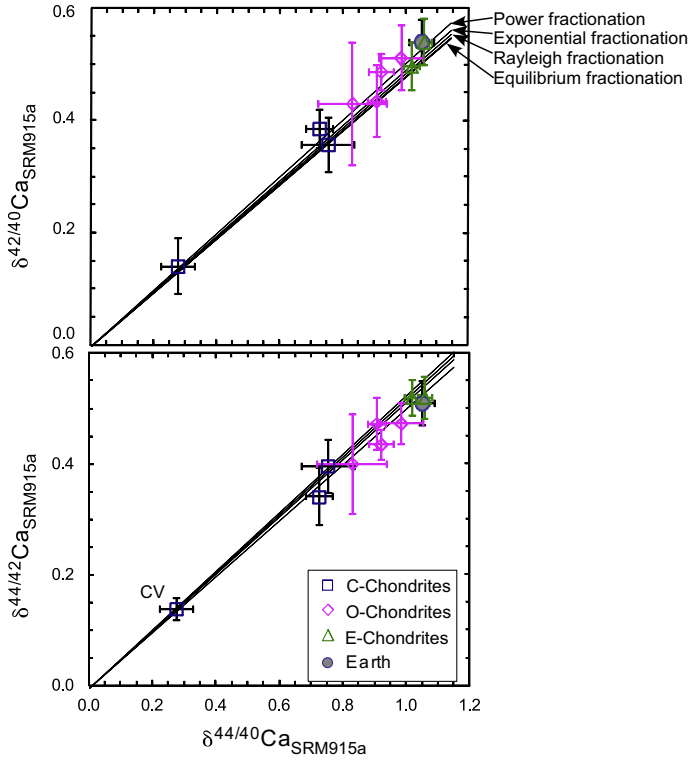

Fig. 2. Calcium three-isotope plots for chondrites, $\delta^{44/40}$Ca vs. $\delta^{42/40}$Ca and $\delta^{44/42}$Ca. The calculated mass-dependent fractionation trends are shown for comparison. Within analytical uncertainty, all chondrites plot on the mass-dependent fractionation trends. In detail, the limited isotopic variation within the chondrites does not allow a discrimination of different mass-dependent fractionation laws (Zhang et al., 2014). Estimates of Earth are from Huang et al. (2010). Two enstatite chondrites have been corrected for small radiogenic ^{40}Ca ingrowth (~0.1 δ-unit) due to their high K/Ca ratios (see also Simon and DePaolo, 2010). Note that, the estimated radiogenic ^{40}Ca ingrowth in enstatite chondrites based on K/Ca ratio is comparable to our analytical uncertainty of unspiked measurement. Carbonaceous chondrites are clearly distinct from Earth and cannot be representative of the Ca in the Earth.

b. Enstatite chondrites: Except for Indarch, the enstatite chondrite $\delta^{44/40}$Ca values from Simon and DePaolo (2010), in general, are significantly higher than that by Valdes et al. (2014) and this study, which agree well. The enstatite chondrites measured by Simon and DePaolo (2010) have been pre-cleaned using water prior to the handling by Simon and DePaolo (2010), which may dissolve oldhamite (CaS), the main Ca carrier in enstatite chondrites. However, the leachate of an enstatite chondrite, Indarch, yields $\delta^{44/40}$Ca of 1.10 (Valdes et al., 2014). Therefore, the origin for the higher enstatite chondrite $\delta^{44/40}$Ca values by Simon and DePaolo (2010) is still unclear. In our following discussion, enstatite chondrite $\delta^{44/40}$Ca values by Simon and DePaolo (2010) are not included.
c. CI chondrites: Orgueil has been measured by Valdes et al. (2014) and in this study, which yield similar $\delta^{44/40}$Ca (0.65 ± 0.05 vs. 0.75 ± 0.08) (Fig. 3a). However, Ivuna measured by Schiller et al. (2015) has $\delta^{44/40}$Ca of 1.13 ± 0.09. Since this is the only chondrite studied by Schiller et al. (2015), the origin of the high $\delta^{44/40}$Ca for Ivuna is unclear.

Fig. 3b shows a comparison of our mass-independent Ca isotopic effects with published values (Simon et al., 2009; Moynier et al., 2010; Chen et al., 2011; Dauphas et al., 2014; Schiller et al., 2015). In general, there are good agreements among results from different groups. Except for one ordinary chondrite Dhajala, at ±1 ε-unit level, there is no measureable $\varepsilon^{40/44}$Ca variation in measured chondrites. At ±2 ε-unit level, there is no measureable $\varepsilon^{43/44}$Ca variation in all measured chondrites. At ±1 ε-unit level, there is no measurable $\varepsilon^{48/44}$Ca variation in all measured ordinary and enstatite chondrites. However, all measured carbonaceous chondrites, except for Allende measured by Moynier et al. (2010), have $\varepsilon^{48/44}$Ca of 2–4. Allende measured in this study has $\varepsilon^{48/44}$Ca of 2.9 ± 0.6. In contrast, Allende measured by Moynier et al. (2010) has $\varepsilon^{48/44}$Ca of 0.0 ± 0.8, which is not included in our following discussion.

4.2. Mass-dependent and mass-independent Ca isotopic variations in bulk chondrites

Spike and unspiked Ca isotopic measurements show that Ca exhibits both mass-dependent and mass-independent isotopic variations in both bulk chondrites and their

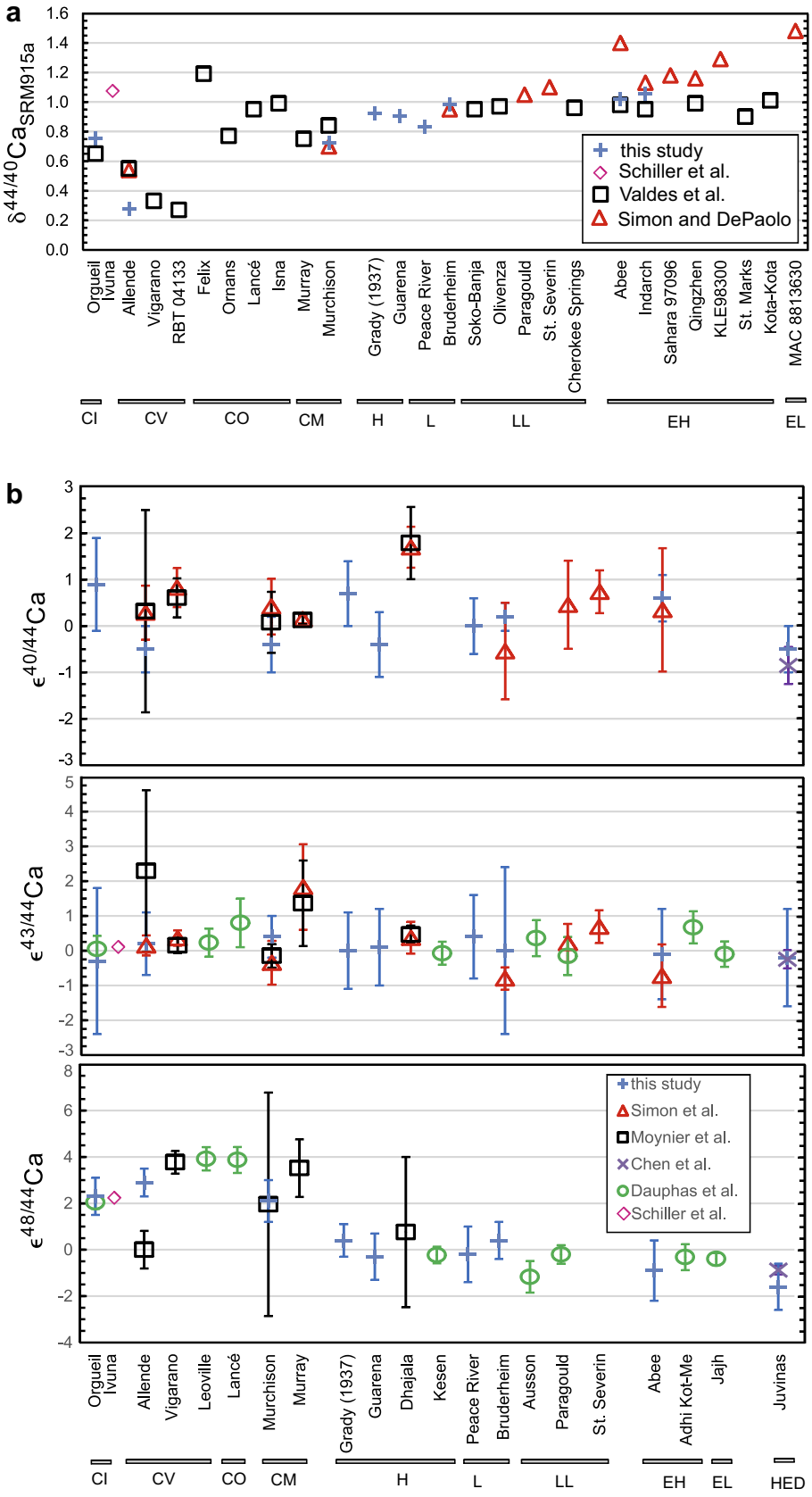

Fig. 3. (a) Comparison of published $\delta^{40/44}$Ca values in chondrites. All values are re-normalized to SRM 915a. (b) Comparison of published $\varepsilon^{40/44}$Ca, $\varepsilon^{43/44}$Ca and $\varepsilon^{48/44}$Ca in chondrites and a eucrite, Juvinas.

components, refractory inclusions (Fig. 4). In detail, refractory inclusions have much larger isotopic variations, both mass-dependent and mass-independent, than bulk chondrites, and they define different fields in this $\delta^{44/40}Ca_{SRM915a}$ vs. $\varepsilon^{48/44}Ca$ diagram (Fig. 4b). This makes Ca the only major element other than O which shows both type of isotopic variations in chondrites and their components.

4.3. Isotopic and chemical variations within chondrites and their relationship to the Earth

Chondrites are primitive meteorites that escaped parental body differentiation processes; however, they exhibit large chemical and isotopic (up to per mil level) variations. Jagoutz et al. (1979) showed that chondrites form a positive Al/Si vs. Mg/Si trend, at a high angle with the negative trend defined by terrestrial peridotites. The negative terrestrial trend is controlled by partial melting, because Al is incompatible and Mg is compatible during partial melting. The positive chondrite trend was suggested to reflect "cosmochemical fractionation" by Jagoutz et al. (1979), which might reflect that the element volatility increases in the order of Al < Mg < Si (e.g., Petaev and Wood, 1998; Lodders, 2003). However, Drake and Righter (2002) termed this trend as "an unexplained trend". Dauphas et al. (2015) showed that within chondrites, Mg/Si ratio is positively correlated with $\delta^{30}Si$. They interpreted this trend as a result of removal of solid olivine from the Solar nebula. Traditionally, the plot of Al/Si vs. Mg/Si is used to constrain the composition of the Earth. That is, the Earth's composition is believed to be at the intersection between the negative terrestrial peridotite trend and the positive

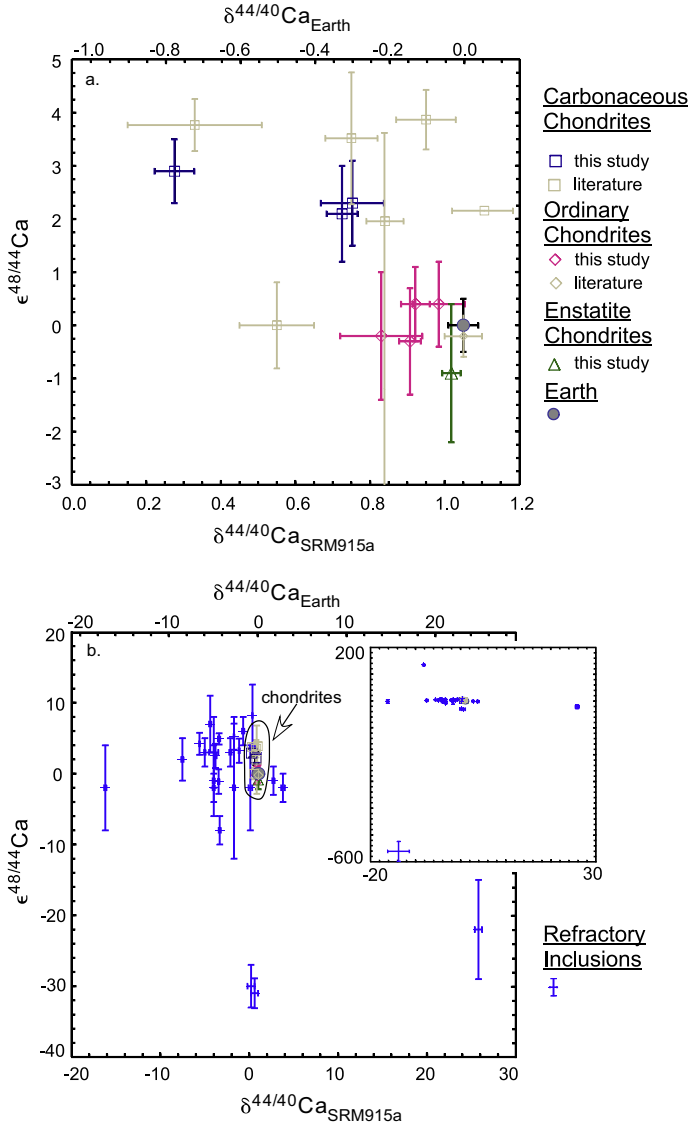

Fig. 4. (a) $\delta^{44/40}Ca$ vs. $\varepsilon^{48/44}Ca$ for chondrites. Data are from Simon et al. (2009), Moynier et al. (2010), Simon and DePaolo (2010), Valdes et al. (2014), Schiller et al. (2015) and this study. Estimates of Earth are from Huang et al. (2010). $\delta^{44/40}Ca_{Earth} = \delta^{44/40}Ca_{SRM915a} - 1.05$. (b) $\delta^{44/40}Ca$ vs. $\varepsilon^{48/44}Ca$ for chondrites compared to refractory inclusions. Refractory data are from the compilation of Clayton et al. (1988) and Huang et al. (2012).

chondrite trend, close to where the carbonaceous chondrites plot (e.g., Jagoutz et al., 1979; McDonough and Sun, 1995; Drake and Righter, 2002).

Is there an isotopic-element correlation involving Ca in chondrites, similar to the Mg/Si vs. δ^{30}Si trend identified by Dauphas et al. (2015)? Our chondrite $\delta^{44/40}$Ca data are negatively correlated with Ca/Mg ratios (Fig. 5): carbonaceous chondrites define the high-Ca/Mg and low-$\delta^{44/40}$Ca end, and enstatite chondrites define the low-Ca/Mg and high-$\delta^{44/40}$Ca end. The Earth estimate does not plot on or at the extension of the chondrite trend. However, addition of published $\delta^{44/40}$Ca data from Simon and DePaolo (2010), Valdes et al. (2014) and Schiller et al. (2015) makes this trend scatter, because of the high $\delta^{44/40}$Ca values from CO chondrites (Fig. 3a). Particularly, CO3 Felix has $\delta^{44/40}$Ca of 1.2. Excluding the enstatite chondrites studied by Simon and DePaolo (2010) (see Section 4.1), this is the highest $\delta^{44/40}$Ca among all chondrites studied so far (Fig. 3a).

What caused such Ca/Mg vs. $\delta^{44/40}$Ca correlation in chondrites? Most refractory inclusions, especially the ones with Group II rare earth element (REE) patterns, are characterized by low $\delta^{44/40}$Ca (e.g., Huang et al., 2012; Fig. 4), and they are also enriched in Ca and Al relative to Si and Mg (e.g., MacPherson, 2004). They can be one possible candidate for the high-Ca/Mg and low-$\delta^{44/40}$Ca endmember. Consistent with this interpretation is the Ca isotopic and REE elemental differences between CV3 Allende and CI1 Orgueil. CV3 Allende has a lower $\delta^{44/40}$Ca than CI1 Orgueil (Fig. 3a), and it has been known that compared to Orgueil, Allende has a Group II REE pattern (e.g., Pourmand et al., 2012; Barrat et al., 2012; Dauphas and Pourmand, 2015). Huang et al. (2012) showed that refractory inclusions with Group II REE patterns have much lower $\delta^{44/40}$Ca than those with unfractionated REE patterns and the bulk Earth estimate. However, CI Orgueil has $\delta^{44/40}$Ca lower than ordinary and enstatites chondrites (Fig. 3a), and it only contains negligible amount of refractory inclusions (Hezel et al., 2008). Therefore, in addition to refractory inclusions, the $\delta^{44/40}$Ca variation in chondrites must have other origins. For example, Simon and DePaolo (2010) proposed that kinetic effect caused by supercooling occurred during Solar nebular condensation might play a role fractionating Ca isotopes.

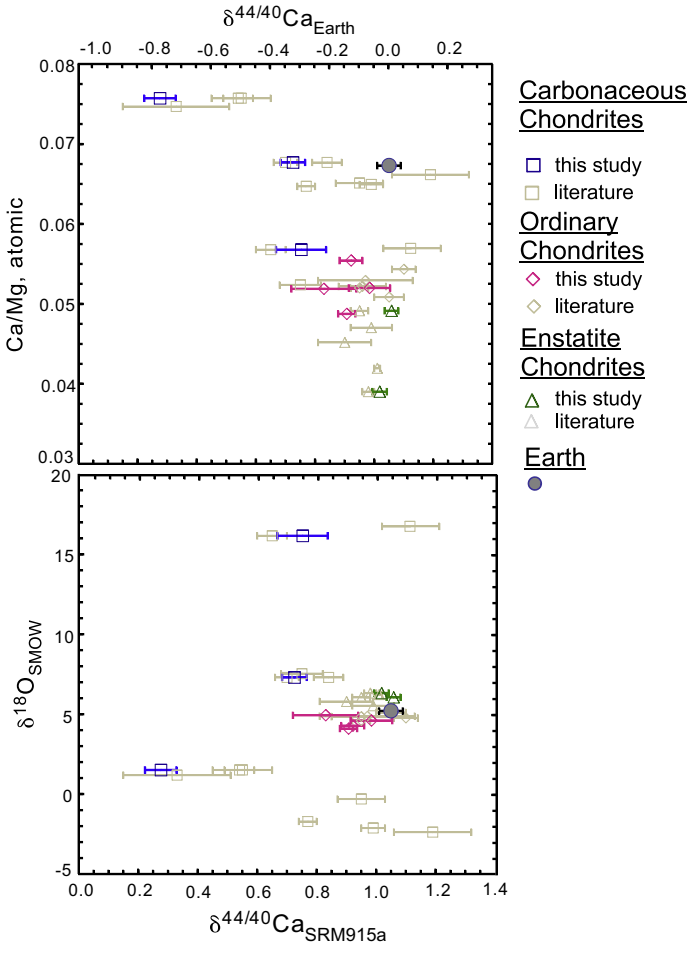

Fig. 5. $\delta^{44/40}$Ca vs. Ca/Mg and δ^{18}O for chondrites. Ca data from this study are shown in color, and they form a negative $\delta^{44/40}$Ca vs. Ca/Mg trend. Literature data are shown in grey. Ca data are from Fig. 3. Elemental data are from Mason (1966), Baadsgaard et al. (1964), Jarosewich and Mason (1969), Kallemeyn and Wasson (1981, 1986), Grossman et al. (1985), Anders and Grevesse (1989), Kallemeyn et al. (1989), and Jarosewich (1990). Oxygen data are from Clayton et al. (1991), Clayton and Mayeda (1999), Newton et al. (2000), and Herd et al. (2013). Estimates of Earth are from McDonough and Sun (1995) and Huang et al. (2010).

In a $\delta^{44/40}$Ca vs. Ca/Mg plot, the Earth plots close to CO chondrites; however, carbonaceous chondrites have very different δ^{18}O than the Earth (Fig. 5), implying that the processes that made the Earth are fundamentally different from those that made the chondrites. It is now well established that the Earth and enstatite chondrites share almost the same isotopic characteristics (e.g., Figs. 2 and 4–6; Clayton, 2003 for O; this study for Ca; see summary in Huang et al., 2013 for ^{142}Nd; see Kaminski and Javoy, 2013 for a more complete summary), but they have different chemical compositions (e.g., Fig. 5; Jagoutz et al., 1979; Wasson and Kallemeyn, 1988; Jarosewich, 1990; Drake and Righter, 2002). In order to explain the chemical difference between Earth and enstatite chondrites, Jacobsen et al. (2013) proposed that the Earth and the enstatite chondrites formed from the same parental nebular reservoir, but experienced different condensation processes. Specifically, enstatite chondrites formed in an H-poor environment with high f_{S2} (at Fe–FeS buffer) and low f_{O2} (at CO–CO_2 buffer) (e.g., Lehner et al., 2013).

4.4. Correlations among neutron-rich isotopes in bulk chondrites: ^{48}Ca, ^{50}Ti and ^{54}Cr

The nucleosynthetic origin of ^{48}Ca is not fully understood. It has 28 neutrons and 20 protons; consequently, it requires special neutron-rich processes (e.g., Cameron, 1979) during Type Ia supernova explosion (Meyer et al., 1996; Woosley, 1997) and electron-capture supernova explosion (Wanajo et al., 2013). Large ^{48}Ca excess has been first observed in FUN CAI EK 1-4-1 (Lee et al., 1978, 1979), and HAL-like hibonites are found to have negative ^{48}Ca anomalies (Lee et al., 1979; Ireland et al., 1992). Subsequent studies on refractory inclusions and bulk carbonaceous chondrites also revealed several ε-units of ^{48}Ca excess (Jungck et al., 1984; Niederer and Papanastassiou, 1984; Moynier et al., 2010; Huang et al., 2012; this study; Fig. 4).

More recent studies also reported nucleosynthetic anomalies of ^{50}Ti and ^{54}Cr, another two neutron-rich isotopes, in bulk chondrites (e.g., Trinquier et al., 2007, 2008, 2009; Leya et al., 2008; Yin et al., 2009; Dauphas et al., 2010; Qin et al., 2010; Zhang et al., 2012). As shown in a summary diagram (Warren, 2011 following Yin et al., 2009), carbonaceous chondrites form a negative ε^{54}Cr vs. ε^{50}Ti trend, and ordinary and enstatite chondrites and other differentiated meteorites form a positive ε^{54}Cr vs. ε^{50}Ti trend, implying that at least three endmembers are required for these two neutron-rich isotopes. ^{48}Ca data also add to the story (Dauphas et al., 2014; Fig. 6). Dauphas et al. (2014) showed that bulk meteorites define a linear trend in a plot of $\varepsilon^{48/44}$Ca vs. ε^{50}Ti. We found that new measurements from CM chondrites also plot on this chondrite trend

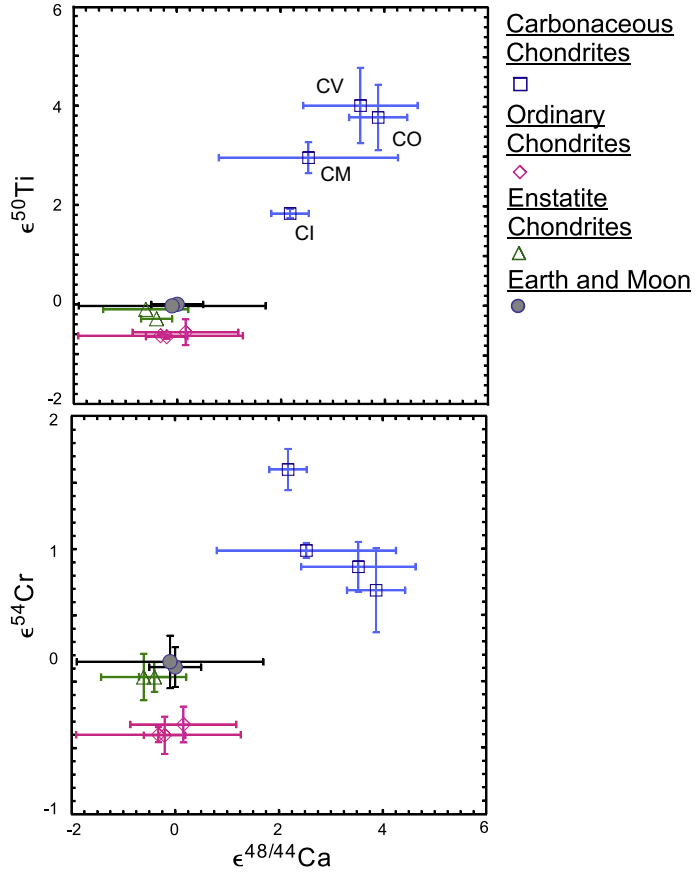

Fig. 6. Relationship among nucleosynthetic anomalies in neutron-rich isotopes, ^{48}Ca, ^{50}Ti and ^{54}Cr, in chondrites. Similar to Dauphas et al. (2014), group averages are plotted. Ca data are from Fig. 3; Ti data are from Leya et al., 2008; Trinquier et al., 2009; Zhang et al., 2012; and Cr data are from Trinquier et al., 2007, 2008; Qin et al., 2010.

(Fig. 6a). CV and CO chondrites define the high $\varepsilon^{48/44}$Ca and ε^{50}Ti end of this chondrite trend. Earth and enstatite chondrites have essentially the same $\varepsilon^{48/44}$Ca and ε^{50}Ti. Compared to Earth and enstatite chondrites, ordinary chondrites have unresolvable $\varepsilon^{48/44}$Ca, but slightly lower ε^{50}Ti.

In a plot of $\varepsilon^{48/44}$Ca vs. ε^{54}Cr, clearly at least three endmembers can be inferred (Fig. 6). Carbonaceous chondrites form a negative $\varepsilon^{48/44}$Ca vs. ε^{54}Cr trend. Earth, enstatite chondrites and ordinary chondrites form a vertical trend with overlapping $\varepsilon^{48/44}$Ca but variable ε^{54}Cr. Compared to Earth and enstatite chondrites, ordinary chondrites have the same $\varepsilon^{48/44}$Ca, but lower ε^{54}Cr.

Chen et al. (2011) studied the relationship of $\varepsilon^{48/44}$Ca vs. ε^{50}Ti and ε^{54}Cr in differentiated meteorites, and they concluded that the observed isotopic anomalies in neutron-rich isotopes, ^{48}Ca, ^{50}Ti and ^{54}Cr, reflect contributions from a rare subset of neutron-rich Type Ia supernova. In fact, ejecta from Type Ia (Woosley, 1997) and electron-capture supernova explosions (Wanajo et al., 2013) could have variable ε^{50}Ti/$\varepsilon^{48/44}$Ca and ε^{54}Cr/$\varepsilon^{48/44}$Ca according to their different ignition density conditions. Although Dauphas et al. (2014) emphasized on the linearity of the $\varepsilon^{48/44}$Ca vs. ε^{50}Ti trend formed by chondrites, the relationship among chondrites in a plot of $\varepsilon^{48/44}$Ca vs. ε^{54}Cr clearly demonstrates that at least three endmembers are required for the neutron-rich isotopic anomalies (Warren, 2011; Fig. 6), assuming these endmembers have similar Cr/Ca ratios. If this is the case, it is highly likely that these neutron-rich isotopes have multiple supernova origins. Alternatively, the $\varepsilon^{48/44}$Ca vs. ε^{54}Cr relationship in chondrites may also be explained by two isotopic endmembers, which could have variable Cr/Ca ratios during condensation, because Cr is more volatile than the highly refractory Ti and Ca (e.g., Lodders, 2003). In this circumstance, multiple supernova origins are not required for ^{48}Ca, ^{50}Ti and ^{54}Cr in chondrites.

4.5. Correlation between ^{48}Ca anomaly and mass-independent O isotopic variation

The origin of the mass-independent O isotopic variation has been a puzzle (e.g., Clayton, 2011), and the current most popular interpretation is the "self-shielding" model, a photochemical process (e.g., Thiemens and Heidenreich, 1983; Clayton, 2002; Lyons and Young, 2005). Consequently, mass-independent O isotopic variation, Δ^{17}O, is not expected to be correlated with nucleosynthetic anomalies. However, Trinquier et al. (2007), Yin et al. (2009) and Warren (2011) showed nice correlation between Δ^{17}O and ε^{54}Cr. In detail, carbonaceous chondrites as one group, and enstatite and ordinary chondrites and differentiated meteorites as another group form two subparallel, positive Δ^{17}O–ε^{54}Cr trends. Interestingly, such correlation is also extended to ^{48}Ca (Fig. 7). Primitive and differentiated chondrites form a "n" shape in a plot of $\varepsilon^{48/44}$Ca vs. Δ^{17}O: the left leg is formed of differentiated meteorites, the right leg is formed of carbonaceous chondrites, and they are bridged by Earth–Moon, Mars, ordinary and enstatite chondrites. That is, any meteorites with negative Δ^{17}O show some ^{48}Ca anomaly, either positive or negative. It is possible that the CO self-shielding process that generated the Δ^{17}O variations in the Solar System occurred after the neutron-rich isotopes were delivered to the Solar System and before they were completely homogenized. Alternatively, this type of correlation between nucleosynthetic anomalies and Δ^{17}O (Trinquier et al., 2007; Yin et al., 2009; Warren, 2011; Fig. 7) implies that Δ^{17}O variation in the Solar System may reflect variable contribution from a ^{16}O-poor carrier (s) (Krot et al., 2010; Kööp et al., 2016a,b), i.e., nucleosynthetic origin.

An interesting question is where the Sun plots in this diagram. The Sun has a very negative Δ^{17}O at about −30 (McKeegan et al., 2011). If the Sun plots on the carbonaceous chondrite trend, it is predicted to have ^{48}Ca excess.

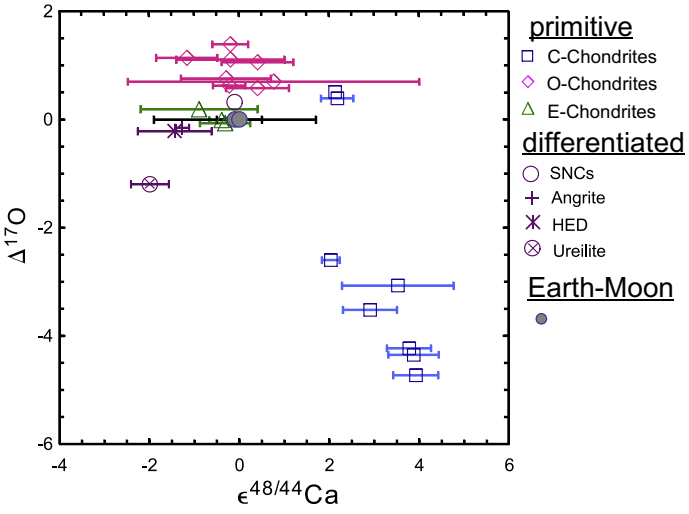

Fig. 7. $\varepsilon^{48/44}$Ca vs. Δ^{17}O for primitive and differentiated meteorites. They form an "n" shape in this plot, with one leg consisting of carbonaceous chondrites, another of differentiated meteorites, and bridged by planets (Earth, Moon, and Mars) and ordinary and enstatite chondrites. Ca data are from Chen et al. (2011), Dauphas et al. (2014), Schiller et al. (2015) and Fig. 3; O data are from Clayton and Mayeda (1996), Franchi et al. (1999), Clayton (2003), Wiechert et al. (2004).

If it plots on the differentiated meteorite trend, then it should be characterized by ^{48}Ca deficit. Since the Solar System is dominated by the Sun, the exact ^{48}Ca anomaly of the Sun provides important constraint on the amount of supernova material that contaminated the Solar nebular.

5. SUMMARY

1. There is ~1‰ $\delta^{44/40}$Ca variation within chondrites, which is comparable to that reported for terrestrial silicate rocks (Fantle and Tipper, 2014), and twice as that reported for martian meteorites (Magna et al., 2015). $\delta^{44/40}$Ca variation in chondrites has multiple origins.
2. At ±1 and ±2 ε-unit levels, respectively, there is no measurable ^{40}Ca or ^{43}Ca anomaly in chondrites, the Moon and a eucrite. Up to several ε-units of ^{48}Ca anomalies have been observed in carbonaceous chondrites (positive) and differentiated meteorites (most negative).
3. Relationship among neutron-rich isotopes (^{48}Ca, ^{50}Ti and ^{54}Cr) in chondrites imply that they may have multiple supernova origins;
4. The Earth and enstatite chondrites share almost the same isotopic signatures, but different chemical compositions. It is possible that they originated from the same parental nebular reservoir but experienced different condensation paths.
5. The relationship between mass-independent O isotopic variations and nucleosynthetic anomalies in neutron-rich isotopes may yield important constraint on the timing of the CO self-shielding process. Alternatively, the Δ^{17}O variation within the Solar System may have a nucleosynthetic origin (Krot et al., 2010; Kööp et al., 2016a,b).
6. The Sun is predicted to have either ^{48}Ca excess or deficit compared to the Earth, and presumably all other neutron-rich isotopes, such as ^{50}Ti and ^{54}Cr.
7. CAIs cannot be taken as representative of the initial isotopic compositions of refractory elements like Ca for the Earth–Moon system.

ACKNOWLEDGEMENT

This work was supported by NASA Cosmochemistry Grants NNX12AH65G and NNX15AH66G. We thank constructive reviews from A. M. Davis, C. D. Williams and J. I. Simon, and editorial handling by Q.-Z. Yin.

REFERENCES

Amini M., Eisenhauer A., Böhm F., Holmden C., Kreissig K., Hauff F. and Jochum K. P. (2009) Calcium isotopes ($\delta^{44/40}$Ca) in MPI-DING reference glasses, USGS rock powders and various rocks: evidence for Ca isotope fractionation in terrestrial silicates. *Geostand. Newsl.* **33**, 231–247.

Anders E. and Grevesse N. (1989) Abundances of the elements: meteoritic and solar. *Geochim. Cosmochim. Acta* **53**, 197–214.

Armytage R. M. G., Georg R. B., Savage P. S., Williams H. and Halliday A. N. (2011) Silicon isotopes in meteorites and planetary core formation. *Geochim. Cosmochim. Acta* **75**, 3662–3676.

Baadsgaard H., Folinsbee R. E. and Cumming G. L. (1964) Peace River meteorite. *J. Geophys. Res.* **69**, 4197–4200.

Barrat J. A., Zanda B., Moynier F., Bollinger C., Liorzou C. and Bayon G. (2012) Geochemistry of CI chondrites: Major and trace elements, and Cu and Zn isotopes. *Geochim. Cosmochim. Acta* **83**, 79–92.

Burbidge E. A., Burbidge G. R., Fowler W. A. and Hoyle F. (1957) Synthesis of the elements in stars. *Rev. Mod. Phys.* **29**, 547–650.

Cameron A. G. W. (1979) The neutron-rich silicon-burning and equilibrium processes of nucleosynthesis. *Astrophys. J.* **230**, L53–L57.

Caro G., Papanastassiou D. A. and Wasserburg G. J. (2010) ^{40}K–^{40}Ca isotopic constraints on the oceanic calcium cycles. *Earth Planet. Sci. Lett.* **296**, 124–132.

Chakrabarti R. and Jacobsen S. B. (2010a) The isotopic composition of magnesium in the inner Solar System. *Earth Planet. Sci. Lett.* **293**, 349–358.

Chakrabarti R. and Jacobsen S. B. (2010b) Silicon isotopes in the inner Solar System: Implications for core formation, solar nebular processes and partial melting. *Geochim. Cosmochim. Acta* **74**, 6921–6933.

Chen H.-W., Lee T., Lee D.-C., Shen J. J.-S. and Chen J.-C. (2011) ^{48}Ca heterogeneity in differentiated meteorites. *Astrophys. J.* **743**(L23), 5.

Clayton R. N. (2002) Solar System: Self-shielding in the solar nebula. *Nature* **415**, 860–861.

Clayton R. N. (2003) Oxygen isotopes in the Solar System. *Space Sci. Rev.* **106**, 19–32.

Clayton R. N. (2011) The Earth and the Sun. *Science* **332**, 1509–1510.

Clayton R. N. and Mayeda T. K. (1996) Oxygen isotope studies of achondrites. *Geochim. Cosmochim. Acta* **60**, 1999–2017.

Clayton R. N. and Mayeda T. K. (1999) Oxygen isotope studies of carbonaceous chondrites. *Geochim. Cosmochim. Acta* **63**, 2089–2104.

Clayton R. N., Hinton R. W. and Davis A. M. (1988) Isotopic variations in the rock-forming elements in meteorites. *Phil. Trans. R. Soc. Lond. A* **325**, 483–501.

Clayton R. N., Mayeda T. K., Goswami J. N. and Olsen E. J. (1991) Oxygen isotope studies of ordinary chondrites. *Geochim. Cosmochim. Acta* **55**, 2317–2337.

Dauphas N., Remusat L., Chen J.-H., Roskosz M., Papanastassiou D. A., Stodolna J., Guan Y., Ma C. and Eiler J. M. (2010) Neutron-rich chromium isotope anomalies in supernova nanoparticles. *Astrophys. J.* **720**, 1577–1591.

Dauphas N., Chen J. H., Zhang J., Papanastassiou D. A., Davis A. M. and Travaglio C. (2014) Calcium-48 isotopic anomalies in bulk chondrites and achondrites: evidence for a uniform isotopic reservoir in the inner protoplanetary disk. *Earth Planet. Sci. Lett.* **407**, 96–108.

Dauphas N. and Pourmand A. (2015) Thulium anomalies and rare earth element patterns in meteorites and Earth: Nebular fractionation and the nugget effect. *Geochim. Cosmochim. Acta* **163**, 234–261.

Dauphas N., Poitrasson F., Burkhardt C., Kobayashi H. and Kurosawa K. (2015) Planetary and meteoritic Mg/Si and δ^{30}Si variations inherited from solar nebula chemistry. *Earth Planet. Sci. Lett.* **427**, 236–248.

Drake M. J. and Righter K. (2002) Determining the composition of the Earth. *Nature* **416**, 39–44.

Fantle M. S. and Tipper E. T. (2014) Calcium isotopes in the global biogeochemical Ca cycle: Implications for development of a Ca isotope proxy. *Earth-Sci. Rev.* **129**, 148–177.

Fitoussi C. and Bourdon B. (2012) Silicon isotope evidence against an enstatite chondrite Earth. *Science* **335**, 1477–1480.

Fitoussi C., Bourdon B., Kleine T., Oberli F. and Reynolds B. C. (2009) Si isotope systematics of meteorites and terrestrial peridotites: implications for Mg/Si fractionation in the solar nebula and for Si in the Earth's core. *Earth Planet. Sci. Lett.* **287**, 77–85.

Franchi I. A., Wright I. P., Sexton A. S. and Pillinger C. T. (1999) The oxygen-isotopic composition of Earth and Mars. *Meteorit. Planet. Sci.* **34**, 657–661.

Georg R. B., Halliday A. N., Schauble E. A. and Reynolds B. C. (2007) Silicon in the Earth's core. *Nature* **447**, 1102–1106.

Grossman J. N., Rubin A. E., Rambaldi E. R., Rajan R. S. and Wasson J. T. (1985) Chondrules in the Qingzhen type-3 enstatite chondrite: Possible precursor components and comparison to ordinary chondrite chondrules. *Geochim. Cosmochim. Acta* **49**, 1781–1795.

Herd C. D. K., Friedrich J. M., Greenwood R. C. and Franchi I. A. (2013) An igneous-textured clast in the Peace River meteorite: insights into accretion and metamorphism of asteroids in the early solar system. *Can. J. Earth Sci.* **50**, 14–25.

Hezel D. C., Russell S. S., Ross A. J. and Kearsley A. T. (2008) Modal abundances of CAIs: Implications for bulk chondrite element abundances and fractionations. *Meteorit. Planet. Sci.* **43**, 1879–1894.

Huang S., Farkaš J. and Jacobsen S. B. (2010) Calcium isotopic fractionation between clinopyroxene and orthopyroxene from mantle peridotites. *Earth Planet. Sci. Lett.* **292**, 337–344.

Huang S., Farkaš J. and Jacobsen S. B. (2011) Stable calcium isotopic compositions of Hawaiian shield lavas: Evidence for recycling of ancient marine carbonates into the mantle. *Geochim. Cosmochim. Acta* **75**, 4987–4997.

Huang S., Farkaš J., Yu G., Petaev M. I. and Jacobsen S. B. (2012) Calcium isotopic ratios and rare earth element abundances in refractory inclusions from Allende CV3 chondrite. *Geochim. Cosmochim. Acta* **77**, 252–265.

Huang S., Jacobsen S. B. and Mukhopadhyay S. (2013) ^{147}Sm-^{143}Nd systematics of Earth are inconsistent with a superchondritic Sm/Nd ratio. *Proc. Natl. Acad. Sci. USA* **110**, 4929–4934.

Huang F., Wu Z., Huang S. and Wu F. (2014) First-principles calculations of equilibrium silicon isotope fractionation among mantle minerals. *Geochim. Cosmochim. Acta* **140**, 509–520.

Ireland T. R., Zinner E. K., Fahey A. J. and Esat T. M. (1992) Evidence for distillation in the formation of HAL and related hibonite inclusions. *Geochim. Cosmochim. Acta* **56**, 2503–2520.

Jacobsen S. B. and Wasserburg G. J. (1980) Sm-Nd isotopic evolution of chondrites. *Earth Planet. Sci. Lett.* **50**, 139–155.

Jacobsen S. B., Petaev M., Huang S. and Sasselov D. (2013) An isotopically homogeneous inner terrestrial planet region. *Mineral. Mag.* **77**(5), 1371.

Jagoutz E., Palme H., Baddenhausen H., Blum K., Cendales M., Dreibus G., Spettel B. and Lorenz V. (1979) The abundances of major, minor and trace elements in the earth's mantle as derived from primitive ultramafic nodules. *Proc. Lunar Planet. Sci. Conf.* **10**, 2031–2050.

Jarosewich E. (1990) Chemical analyses of meteorites: a compilation of stony and iron meteorite analyses. *Meteoritics* **25**, 323–337.

Jarosewich E. and Mason B. (1969) Chemical analyses with notes on one mesosiderite and seven chondrites. *Geochim. Cosmochim. Acta* **33**, 411–416.

Jungck M. H. A., Shimamura T. and Lugmair G. A. (1984) Ca isotope variation in Allende. *Geochim. Cosmochim. Acta* **48**, 2651–2658.

Kallemeyn G. W. and Wasson J. T. (1981) The compositional classification of chondrites: I. The carbonaceous chondrite groups. *Geochim. Cosmochim. Acta* **45**, 1217–1230.

Kallemeyn G. W. and Wasson J. T. (1986) Compositions of enstatite (EH3, EH4,5 and EL6) chondrites: Implications regarding their formation. *Geochim. Cosmochim. Acta* **50**, 2153–2164.

Kallemeyn G. W., Rubin A. E., Wang D. and Wasson J. T. (1989) Ordinary chondrites: Bulk compositions, classification, lithophile-element fractionations, and composition-petrographic type relationships. *Geochim. Cosmochim. Acta* **53**, 2747–2767.

Kaminski E. and Javoy M. (2013) A two-stage scenario for the formation of the Earth's mantle and core. *Earth Planet. Sci. Lett.* **365**, 97–107.

Kööp L., Nakashima D., Heck P. R., Kita N. T., Tenner T. J., Krot A. N., Nagashima K., Park C. and Davis A. M. (2016a) New constraints on the relationship between ^{26}Al and oxygen, calcium, and titanium isotopic variation in the early Solar System from a multielement isotopic study of spinel-hibonite inclusions. *Geochim. Cosmochim. Acta* **184**, 151–172.

Kööp L., Davis A. M., Nakashima D., Park C., Krot A. N., Nagashima K., Tenner T. J., Heck P. R. and Kita N. T. (2016b) A link between oxygen, calcium and titanium isotopes in ^{26}Al-poor hibonite-rich CAIs from Murchison and implications for the heterogeneity of dust reservoirs in the solar nebula. *Geochim. Cosmochim. Acta* **189**, 70–95.

Krot A. N., Nagashima K., Ciesla F. J., Meyer B. S., Hutcheon I. D., Davis A. M., Huss G. R. and Scott E. R. D. (2010) Oxygen isotopic composition of the Sun and mean oxygen isotopic composition of the protosolar silicate dust: Evidence from refractory inclusion. *Astrophys. J.* **713**, 1159–1166.

Lee T., Papanastassiou D. A. and Wasserburg G. J. (1978) Calcium isotopic anomalies in the Allende meteorite. *Astrophys. J.* **220**, L21–L25.

Lee T., Russell W. A. and Wasserburg G. J. (1979) Calcium isotopic anomalies and the lack of aluminium-26 in an unusual Allende inclusion. *Astrophys. J.* **228**, L93–L98.

Lehner S. W., Petaev M. I., Zolotov M. Yu. and Buseck P. R. (2013) Formation of niningerite by silicate sulfidation in EH3 enstatite chondrite. *Geochim. Cosmochim. Acta* **101**, 34–56.

Leya I., Schoenbachler M., Wiechert U., Krahenbuhl U. and Halliday A. N. (2008) Titanium isotopes and the radial heterogeneity of the solar system. *Earth Planet. Sci. Lett.* **266**, 233–244.

Lodders K. (2003) Solar system abundances and condensation temperatures of the elements. *Astrophys. J.* **591**, 1220–1247.

Lyons J. R. and Young E. D. (2005) CO self-shielding as the origin of oxygen isotope anomalies in the early solar nebula. *Nature* **435**, 317–320.

MacPherson G. J. (2004) Calcium-aluminium-rich inclusions in chondritic meteorites. In *Treaties on Geochemistry*, 1 (ed. A. M. Davis). Elsevier, pp. 201–246.

Magna T., Gussone N. and Mezger K. (2015) The calcium isotope systematics of Mars. *Earth Planet. Sci. Lett.* **430**, 86–94.

Mason B. (1966) The enstatite chondrites. *Geochim. Cosmochim. Acta* **30**, 23–39.

Meyer B. S., Krishnan T. D. and Clayton D. D. (1996) ^{48}Ca production in matter expanding from high temperature and density. *Astrophys. J.* **462**, 825–838.

McDonough W. F. and Sun S.-S. (1995) Composition of the Earth. *Chem. Geol.* **120**, 223-153.

McKeegan K. D., Kallio A. P. A., Heber V. S., Jarzebinski G., Mao P. H., Coath C. D., Kunihiro T., Wiens R. C., Nordholt J. E., Moses, Jr., R. W., Reisenfeld D. B., Jurewicz A. J. G. and Burnett D. S. (2011) The oxygen isotopic composition od the Sun inferred from captured Solar wind. *Science* **332**, 1528–1532.

Moynier F., Simon J. I., Podosek F. A., Meyer B. S., Brannon J. and DePaolo D. J. (2010) Ca isotope effects in Orgueil leachates and the implications for the carrier phases of ^{54}Cr anomalies. *Astrophys. J.* **718**, L7–L13.

Newton J., Franchi I. A. and Pillinger C. T. (2000) The oxygen-isotopic record in enstatite meteorites. *Meteorit. Planet. Sci.* **35**, 689–698.

Niederer F. R. and Papanastassiou D. A. (1984) Ca isotopes in refractory inclusions. *Geochim. Cosmochim. Acta* **48**, 1279–1293.

Petaev M. I. and Wood J. A. (1998) The condensation with partial isolation (CWPI) model of condensation in the solar nebula. *Meteorit. Planet. Sci.* **33**, 1123–1137.

Poitrasson F., Levasseur S. and Teutsch N. (2005) Significance of iron isotope mineral fractionation in pallasites and iron meteorites for the core-mantle differentiation of terrestrial planets. *Earth Planet. Sci. Lett.* **234**, 151–164.

Pourmand A., Dauphas N. and Ireland T. J. (2012) A novel extraction chromatography and MC-ICP-MS technique for rapid analysis of REE, Sc and Y: Revising CI-chondrite and Post-Archean Australian Shale (PAAS) abundances. *Chem. Geol.* **291**, 38–54.

Qin L., Alexander C. M., Carlson R. W., Horan M. F. and Yokoyama T. (2010) Contributors to chromium isotope variation of meteorites. *Geochim. Cosmochim. Acta* **74**, 1122–1145.

Russell W. A., Papanastassiou D. A. and Tombrello T. A. (1978) Ca isotope fractionation on the Earth and other Solar System materials. *Geochim. Cosmochim. Acta* **42**, 1075–1090.

Savage P. S. and Moynier F. (2013) Silicon isotopic variation in enstatite meteorites: clues to their origin and Earth-forming material. *Earth Planet. Sci. Lett.* **361**, 487–496.

Schiller M., Paton C. and Bizzarro M. (2015) Evidence for nucleosynthetic enrichment of the protosolar molecular cloud core by multiple supernova events. *Geochim. Cosmochim. Acta* **149**, 88–102.

Schoenberg R. and von Blanckenburg F. (2006) Modes of planetary-scale Fe isotope fractionation. *Earth Planet. Sci. Lett.* **252**, 342–359.

Shahar A., Hillgren V. J., Young E. D., Fei Y., Macris C. A. and Deng L. (2011) High temperature Si isotope fractionation between iron metal and silicate. *Earth Planet. Sci. Lett.* **75**, 7688–7697.

Simon J. I., DePaolo D. J. and Moynier F. (2009) Calcium isotope composition of meteorites, Earth, and Mars. *Astrophys. J.* **702**, 707–715.

Simon J. I. and DePaolo D. J. (2010) Stable calcium isotopic composition of meteorites and rocky planets. *Earth Planet. Sci. Lett.* **289**, 457–466.

Teng F.-Z., Dauphas N. and Helz R. T. (2008) Iron isotope fractionation during magmatic differentiation in Kilauea Iki lava lake. *Science* **320**, 1620–1622.

Teng F., Li W.-Y., Ke S., Marty B., Dauphas N., Huang S., Wu F.-Y. and Pourmand A. (2010) Magnesium isotopic composition of the Earth and chondrites. *Geochim. Cosmochim. Acta* **74**, 4150–4166.

Thiemens M. H. and Heidenreich H. E. (1983) The mass independent fractionation of oxygen – A novel isotope effect and its cosmochemical implications. *Science* **219**, 1073–1075.

Trinquier A., Birck J. L. and Allègre C. J. (2007) Widespread ^{54}Cr heterogeneity in the inner Solar System. *Astrophys. J.* **655**, 1179–1185.

Trinquier A., Birck J.-L., Allègre C. J., Göpel C. and Ulfbeck D. (2008) ^{53}Mn–^{53}Cr systematics of the early Solar System revisited. *Geochim. Cosmochim. Acta* **72**, 5146–5163.

Trinquier A., Elliott T., Ulfbeck D., Coath C., Krot A. N. and Bizzarro M. (2009) Origin of nucleosynthetic isotope heterogeneity in the Solar protoplanetary disk. *Science* **324**, 374–376.

Valdes M. C., Moreira M., Foriel J. and Moynier F. (2014) The nature of Earth's building blocks as revealed by calcium isotopes. *Earth Planet. Sci. Lett.* **394**, 135–145.

von Strandmann P. A. E. P., Elliott T., Marschall H. R., Coath C., Lai Y.-J., Jeffcoate A. B. and Ionov D. A. (2011) Variations of Li and Mg isotope ratios in bulk chondrites and mantle xenoliths. *Geochim. Cosmochim. Acta* **75**, 5247–5268.

Wanajo S., Janka H.-T. and Müller B. (2013) Electron-capture supernovae as origin of ^{48}Ca. *Astrophys. J.* **767**(L26), 6.

Warren P. H. (2011) Stable-isotopic anomalies and the accretionary assemblage of the Earth and Mars: A subordinate role for carbonaceous chondrites. *Earth Planet. Sci. Lett.* **311**, 93–100.

Wasson J. T. and Kallemeyn G. W. (1988) Compositions of chondrites. *Phil. Trans. R. Soc. Lond. A* **325**, 535–544.

Wiechert U. H., Halliday A. N., Palme H. and Rumble D. (2004) Oxygen isotope evidence for rapid mixing of the HED meteorite parent body. *Earth Planet. Sci. Lett.* **221**, 373–382.

Woosley S. E. (1997) Neutron-rich nucleosynthesis in carbon deflagration supernovae. *Astrophys. J.* **476**, 801–810.

Yin, Q.-Z., Yamashita, K., Yamakawa, A., Tanaka, B., Jacobsen, B., Ebel, D., Hutcheon, I. D. & Nakamura, E. (2009) ^{53}Mn–^{53}Cr systematics of Allende chondrules and a ^{54}Cr–Δ^{17}O correlation in bulk carbonaceous chondrites. Lunar Planet. Sci. Conf. 40, #2006.

Zhang J., Dauphas N., Davis A. M., Leya I. and Fedkin A. (2012) The proto-Earth as a significant source of lunar material. *Nat. Geosci.* **5**, 251–255.

Zhang J., Huang S., Davis A. M., Dauphas N., Hashimoto A. and Jacobsen S. B. (2014) Calcium and titanium isotopic fractionations during evaporation. *Geochim. Cosmochim. Acta* **140**, 365–380.

Ziegler K., Young E. D., Schauble E. A. and Wasson J. T. (2010) Metal-silicate silicon isotope fractionation in enstatite meteorites and constraints on Earth's core formation. *Earth Planet. Sci. Lett.* **295**, 487–496.

Associate editor: Qing-Zhu Yin